Ecological Indicators 178 (2025) 114052

Contents lists available at ScienceDirect

Ecological Indicators

journal homepage: www.elsevier.com/locate/ecolind

Original Articles

Seaward expansion of salt marshes on the largest uninhabited island in Changjiang Estuary over the past two decades

Yaying Lou [a,b], Zhijun Dai [b,*], Xuefei Mei [b], Huabing Shi [a,c], Hui Dong [d], Jinping Cheng [e,*]

[a] Zhuhai-M.U.S.T. Science and Technology Research Institute, Zhuhai, China
[b] State Key Laboratory of Estuarine and Coastal Research, East China Normal University, Shanghai, China
[c] State Key Laboratory of Internet of Things for Smart City and Department of Ocean Science and Technology, University of Macau, Macau
[d] Eastern Navigation Service Center, Maritime Safety Administration, The People's Republic of China, Shanghai, China
[e] Department of Science and Environmental Studies, The Education University of Hong Kong, New Territories, Hong Kong, China

ARTICLE INFO

Keywords:
Wetland dynamics
Salt marsh
Sea level rise
Machine learning
Sediment transport

ABSTRACT

Salt marshes are vital estuarine ecosystems that have experienced significant global declines due to sediment dynamics and rising sea levels. Monitoring the dynamics of these habitats is crucial for elucidating the mechanisms driving such changes. This study investigates the spatiotemporal dynamics of salt marshes on JiuDuan Shoal, the largest uninhabited island in the Changjiang Estuary, from 2002 to 2022. Utilizing advanced machine learning techniques, we analyzed a comprehensive dataset comprising Landsat imagery, hydro-sediment measurements, and localized sea level rise data. The results reveal that salt marshes on JiuDuan Shoal underwent substantial seaward expansion, averaging 3.66 km^2/yr, with vertical accretion rates of 0.15 m/yr. Conversely, bare flats shifted from slight deposition (0.01 m/yr from 2002 to 2014) to erosion (0.07 m/yr from 2014 to 2022). Spatial analyses identified distinct expansion patterns, with the Upper Shoal extending northwestward and the Middle-Lower Shoal expanding southwestward. Notably, enhanced tidal currents facilitated continued sediment deposition despite a more than 70 % decline in fluvial sediment discharge. The hydrodynamic changes from the Deep Waterway Project contribute to the observed spatial variability in salt marsh dynamics. Additionally, the invasion of *Spartina alterniflora* has accelerated the seaward marsh expansion. By elucidating the interplay between hydrodynamic changes and salt marsh resilience, our findings provide crucial insights for conservation strategies to safeguard coastal habitats in the face of ongoing environmental challenges.

1. Introduction

Estuarine salt marshes are critical transition zones for land–ocean interactions that stabilize coastlines, support high biological productivity, and provide essential services to coastal communities, including carbon sequestration, coastal protection, and habitats for fish, invertebrates, and migratory birds (Murray et al., 2019; Fagherazzi et al., 2020). Despite being among the most widespread coastal vegetated ecosystems, global salt marshes have experienced a net loss of approximately 1452.84 km^2 between 2000 and 2019, and this decline is primarily attributed to increasing anthropogenic pressures and the effects of accelerated sea-level rise (Campbell et al., 2022). Meanwhile, remarkable spatial heterogeneity characterizes global salt marsh dynamics. In Europe, Laengner et al., (2019) revealed a net gain of 127.5 km^2 in salt marsh extent between 1986 and 2010. Conversely, the salt marshes in China demonstrated a net loss of 359.27 km^2 from 1985 to 2019, while this trend markedly decelerated in recent decades, with losses diminishing to 22.02 km^2 during the 2000–2019 period (Chen et al., 2022). Recent studies have highlighted a renewed interest in salt marsh restoration and expansion, with some regions, such as the Changjiang Estuary, exhibiting patterns of expansion (Dai, 2021). Monitoring the dynamic changes in salt marshes is crucial for understanding these trends. To elucidate the driving factors behind the fluctuations in salt marsh areas within estuarine environments, it is imperative to systematically observe these changes and investigate the underlying mechanisms.

The stability and dynamics of salt marsh habitats are influenced by multiple factors, including sediment availability, anthropogenic activities, and climate change impacts such as sea level rise. Sediment availability is a fundamental determinant of salt marsh growth (Reed,

* Corresponding authors.
E-mail addresses: zjdai@sklec.ecnu.edu.cn (Z. Dai), jincheng@eduhk.hk (J. Cheng).

https://doi.org/10.1016/j.ecolind.2025.114052
Received 7 April 2025; Received in revised form 13 August 2025; Accepted 13 August 2025
Available online 16 August 2025

1988). For example, the collapse of salt marshes in Venice Lagoon, Italy, has been attributed to insignificant riverine sediment supply (Tognin et al., 2021), while a significant loss of 94 km^2 of marshland over the Chesapeake Bay was primarily due to sediment-starved waters (Schieder et al., 2018). Recent studies propose that estuarine sediment may compensate for upstream sediment deficiencies, supporting salt marsh growth under reduced fluvial sediment conditions, as seen in the Changjiang Estuary (Leonardi et al., 2021). These findings highlight the necessity of a comprehensive analysis of fluvial sediment dynamics and other influencing factors in shaping salt marsh evolution.

Anthropogenic activities, including coastal infrastructure development, land conversion, and invasive species have further altered salt marsh ecosystems (Gedan et al., 2009). For instance, over 200,000 ha of salt marsh were lost in San Francisco Bay due to anthropogenic engineering impacts (Gedan et al., 2009). Contrarily, dredging activities in the Atchafalaya Delta have accelerated salt marsh growth through enhancing sediment supply (Yang et al., 2023), while the artificial cultivation of *Spartina alterniflora* has promoted salt marsh expansion in the Chongming Wetland of the Changjiang Estuary (Ge et al., 2015). Additionally, the invasion of non-native *Spartina anglica C.E. Hubbard* has profoundly affected the salt marsh dynamics in the European Wadden Sea by increasing high marsh zone elevations (Granse et al., 2021). These diverse human activities complicate the dynamics of salt marsh expansion and retreat.

The interplay between sediment deposition and local sea-level rise rates also plays a critical role in salt marsh retreat (Jankowski et al., 2017; Horton et al., 2018; Schuerch et al., 2018). For example, 35 % of salt marshes and bare flats in the Mississippi Delta face degradation under a relative Sea Level Rise rate of 12 ± 8 mm/yr (Jankowski et al., 2017). Horton et al. (2018) estimated that over 80 % of salt marsh in the UK might be at risk by 2100 if sea level rise reaches 18 mm/yr. However, Kirwan et al. (2016) argued that these assessments might overstate vulnerability, suggesting that salt marshes along the Gulf and Atlantic coasts of North America and Europe would keep expanding due to internal biophysical feedback mechanisms. This underscores the need for region-specific examinations to better understand salt marsh evolution in response to sea-level rise.

Traditional field observations of salt marsh dynamics are time-consuming and labor-intensive, particularly given their exposure at low tide and submersion at high tide (Chapman, 1960; Murray et al., 2012). The Changjiang Estuary, Asia's largest bifurcated estuary, harbors an extensive salt marshes area (Dai, 2021). JiuDuan Shoal, an uninhabited island within this estuary, presents particular challenges for long-term field studies. However, the availability of remote sensing images offers valuable data for analyzing spatiotemporal changes in salt marshes. Advanced machine learning technique have emerged as an effective method for interpreting remote sensing images (Anthony et al., 2015). This research aims to address gaps in understanding the complex interactions governing salt marsh dynamics. This study aims to utilize Landsat images from 2002 to 2022 by employing machine learning techniques to: 1) quantify variations in the area of JiuDuan Shoal salt marshes; 2) profile the dynamic pattern of these marshes; 3) discern the main driving forces behind their dynamics.

2. Materials and methods

2.1. Study area

As the largest bifurcated estuary in Asia, the Changjiang Estuary features vast expanses of salt marshes, including the Chongming Shoal, Nanhui Shoal, Hengsha Shoal, and JiuDuan Shoal (Fig. 1A and B) (Dai, 2021). Following the operation of the Three Gorges Dam in 2003, the annual fluvial sediment flux in the estuary decreased from 510 to 140 Mt/yr (Luo et al., 2023). Concurrently, the mean sea-level rise in the region has been reported to range from 3 to 28 mm/yr (Wang et al., 2012). Given these evolving environmental conditions and significant anthropogenic influences, considerable changes in the salt marshes of the Changjiang Estuary are anticipated.

JiuDuan Shoal is located in the eastern part of the Changjiang Estuary at the natural bifurcation of the South and North Passages (Chen, 1988) (Fig. 1C). This region is classified as a third-generation newborn island within the estuary (Wei et al., 2017). Historically, JiuDuan Shoal consisted of three distinct shoals: the Upper Shoal, the Middle Shoal, and the Lower Shoal. Over the past two decades, the Middle and Lower Shoal have merged into a single middle-lower shoal (Fig. 1C) (Zhang et al., 2021). The tidal regime near JiuDuan Shoal is characterized by a typical semidiurnal tide. At Zhongjun station, located in the South Passage near the JiuDuan Shoal (Fig. 1), the average tide level is recorded at 2.6 m, with average and maximum tidal ranges of 2.67 m and 4.62 m, respectively (Huang and Zhang, 2007). The salt marsh zone of JiuDuan Shoal is primarily dominated by three vegetation communities: *Phragmites australis*, *Scirpus mariqueter*, and *S. alterniflora* (Lin et al., 2021).

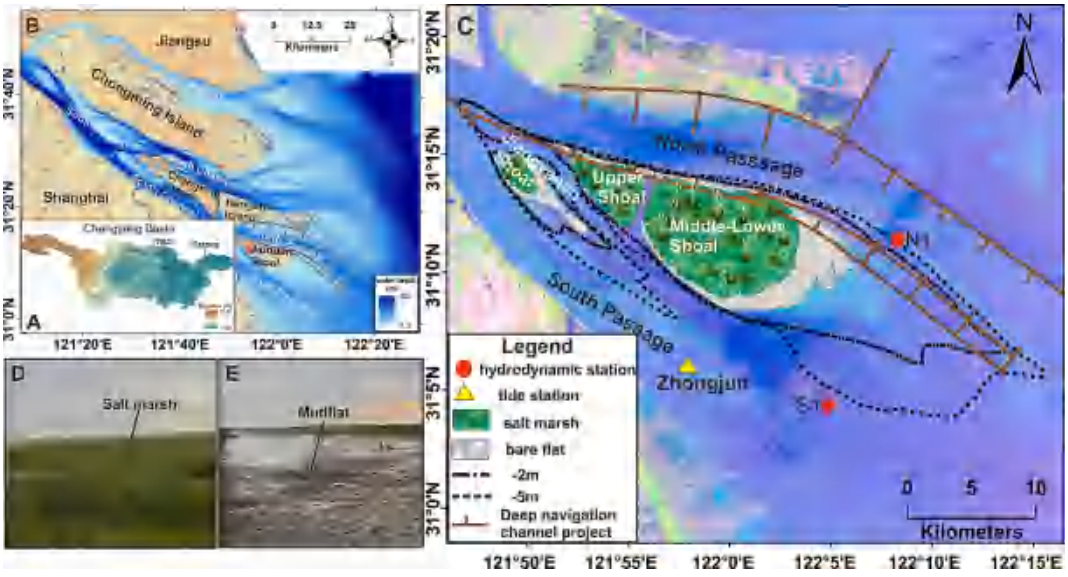

Fig. 1. Geographical Location and Study Area of JiuDuan Shoal within the Changjiang Estuary. A. Map of the Changjiang Basin; B. Map of the Changjiang Estuary; C. Map of the Jiuduan Shoal; D. The salt marsh area in JiuDuan Shoal; E. The bare flat area in JiuDuan Shoal.

These vegetation communities typically inhabit tidal flats with elevations above 2 m, while areas below 2 m are characterized by bare flats (Huang and Zhang, 2007). The Deep Waterway Project, initiated in 1998, is located to the northern of JiuDuan Shoal (Chen et al., 2001). This study focuses on the salt marsh region of JiuDuan Shoal and the adjacent bare flats that are exposed during low tide.

2.2. Data collection

This study utilized two primary datasets. The first dataset comprised 148 Landsat images of JiuDuan Shoal (Path 118, Row 38) captured between 2002 and 2022, which were accessed via the Google Earth Engine (GEE) (https://code.earthengine.google.com/). These Landsat images, with a spatial resolution of 30 m and cloud cover of less than 30 % (Supplementary Fig. S1), were employed to analyze changes in the salt marshes and bare flats of JiuDuan Shoal. The second dataset included hydrological data, including hourly tide levels, tidal currents, and fluvial suspended sediment discharge. Hourly tide level data from Zhongjun Station (2002–2022) were obtained from the China Oceanic Information Network (https://www.coi.gov.cn/). Tidal current data for the representative stations in both the South and North Passage were provided by the Changjiang Estuary Waterway Administration Bureau, Ministry of Transportation of China (CEWAB, https://www.cjkhd.com/). Annual suspended sediment discharge data from 1950 to 2021 were sourced from the Bulletin of China River Sediment (BCRS, https://www.cjh.com.cn/). These datasets provide a comprehensive foundation for analyzing the spatiotemporal dynamics of the JiuDuan Shoal salt marshes.

2.3. Image processing

The random forest algorithm is a robust machine-learning technique frequently employed for remote sensing image classification (Zhang et al., 2019; Yang et al., 2023). In this study, the random forest algorithm was executed on the Google Earth Engine (GEE) platform to classify vegetated tidal flats (salt marshes), unvegetated tidal flats (bare flats), and water bodies, based on their distinct spectral signatures. To enhance spectral differentiation, four water and vegetation indices were utilized: the normalized difference vegetation index (NDVI), modified normalized difference water index (MNDWI), land surface water index (LSWI), and enhanced vegetation index (EVI). The calculation formulas for these indices are provided in Supplementary Table S1. The image processing workflow utilizing Landsat imagery was structured into five steps: (1) removal of cloud and shadow artifacts from the Landsat images; (2) selection of reference samples; (3) calculation of the various water and vegetation indices; (4) classification of Landsat imagery using the random forest algorithm; (5) quantification of the salt marshes and bare flats area within the JiuDuan Shoal tidal flat (Fig. 2).

Reference samples were derived from high-resolution satellite imagery available on Google Earth. Three sample categories-salt marsh, bare flat, and water-were manually delineated through visual interpretation. Using the GEE platform, three thematic layers corresponding to each class were generated and labeled accordingly. Subsequently, training polygons were manually delineated, and 600–800 random points were generated utilizing the 'Random Point' function in GEE. Of these points, 75 % were allocated as training data, while the remaining 25 % were reserved for validation. The random forest algorithm is incorporated as a module of the GEE platform, including six input parameters to define the classifiers (https://code.earthengine.google.com/). To optimize classification accuracy and efficiency, 100 decision trees were established as the optimal parameter for the random forest classifier, while other settings were maintained at their default values.

2.4. Discrimination of Spartina alterniflora

Spartina alterniflora is recognized as an invasive grass species within the salt marshes of the Changjiang Estuary, where it has demonstrated a prominent competitive advantage over native species, leading to its rapid proliferation across the tidal flat (Ge et al., 2020). Consequently, mapping the distribution of *S. alterniflora* in JiuDuan Shoal is essential for understanding changes in salt marshes ecosystems. Notably, *S. alterniflora* exhibits distinct phenological characteristics compared to native species. Ouyang et al. (2013) highlighted that *S. alterniflora* displays varying spectral responses during different growth phases. Specifically, during the green-up stage (April to May), its spectral signal is weaker than that of native vegetation, while in the senescence stage (late October to December), its spectral response becomes more pronounced (Supplementary Fig. S2).

In this study, to analyze *S. alterniflora* distribution, Landsat images captured during the periods of April–May and November–December were specifically selected for analysis (Supplementary Table S2). Three spectral indices-the normalized difference vegetation index, land surface

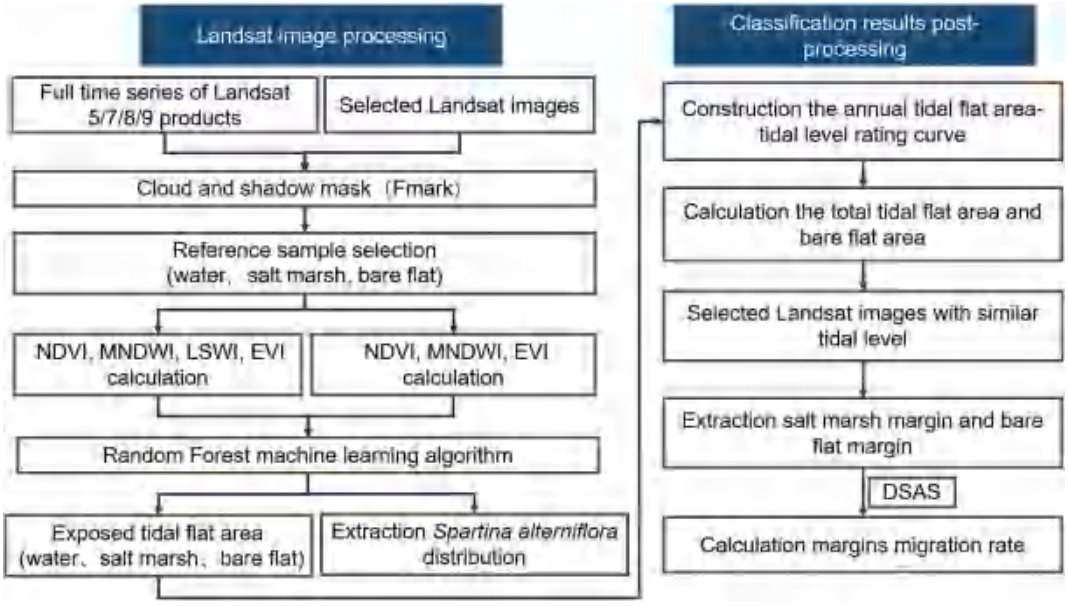

Fig. 2. Workflow of salt marshes and bare flats extraction and classification data post-processing.

water index, and enhanced vegetation index- were employed to discriminate the annual *S. alterniflora* distribution (Supplementary Table S1). In addition, four types of sample points-*S. alterniflora*, native vegetation, bare flat, and water body-were established through visual interpretation. These sample points were then used in conjunction with the random forest algorithm to classify the salt marsh vegetation within JiuDuan Shoal.

2.5. Estimates of salt marshes/bare flats area and elevation

Tidal flats are frequently submerged by tides, making the exposed flat area closely dependent on the instantaneous tide level. To minimize errors caused by variations in tide levels when assessing salt marsh and bare flat areas, tide level–tidal flat area rating curves were developed. The results revealed a remarkable quadratic linear relationship between tide level and both total and bare flats area, with correlation coefficients over 0.95 (Supplementary Figs. S3 and S4). Utilizing the annual quadratic linear fitting formula, the areas of tidal flats and bare flats at a uniform low tide level were calculated. For this analysis, a low tide level of 1.5 m at Zhongjun station was selected as the baseline for evaluating bare flat areas. Additionally, the accretion variations of salt marshes and bare flats in JiuDuan Shoal were recalculated using the following equations:

$$\Delta h = f_{n-1}^{-1}(s_n) - f_n^{-1}(s_n) \quad (1)$$

$$H_n = \sum_{2002}^{n} \Delta h \quad (2)$$

where Δh represents the elevation change of salt marshes/bare flats between two adjacent years; n denotes the year; s_n is the area of salt marshes/bare flats, f_n is the fitting formula correlating tide level with tidal flats or bare flats area. H_n is the total accumulated elevation variation of salt marshes/bare flats during the study period.

The salt marshes and bare flat areas recorded in 2002 served as benchmarks for calculating the accretion rate at JiuDuan Shoal. Supplementary Fig. S5 gives a more intuitive understanding of Eq. (1). The parameter Δh specifically denotes the interannual tidal level difference. Under the assumption of a stable base elevation for salt marshes and bare flats, observed tidal level variations are interpreted as primarily reflecting bed-level adjustments. Furthermore, inherent processes of tidal flats, such as subsidence and soil compaction, exert slight influence on elevation dynamics compared to sedimentation rates (Wang et al., 2012). Consequently, the elevation model simplifies the complexity of tidal flat dynamics, offering a theoretical framework to analyze elevation trends in salt marshes and bare flats. This approach is designed to identify threshold-level elevation changes unique to JiuDuan Shoal, emphasizing critical transitions in its morphodynamic evolution.

To assess changes in salt marshes at JiuDuan Shoal, we selected annual Landsat images acquired under a similar tide level, with the image list shown in Supplementary Table S3. The annual boundaries of salt marshes and bare flats were extracted using ArcGIS. Furthermore, the Digital shoreline analysis system, an extension of ArcGIS, was employed to calculate the total migration distances and annual variation rates of salt marshes and bare flats in JiuDuan Shoal from 2002 to 2022.

2.6. Accuracy evaluation

To ensure the reliability and scientific validity of the processed data regarding salt marshes and bare flats, a comprehensive accuracy evaluation was conducted. This assessment focused on two primary error types: classification errors in Landsat images and numerical calculation errors. Liu et al. (2016) suggested that an error matrix with independent validation samples is a standard method for evaluating the performance of random forest classification algorithms in remote sensing image interpretation. Supplementary Table S4 presents four key indicators to verify the classification accuracy of the Landsat image. Producer accuracy and user accuracy are further divided into three classes, corresponding to three landforms identified in imagery. The overall accuracy and the kappa coefficient (k) serve as primary metrics to evaluate the overall classification performance of images (Jia et al., 2018). The overall accuracies from 2002 to 2022 ranged from 0.969 to 0.998, with the most annual kappa coefficients exceeding 0.95, indicating a high level of confidence in the random forest classification employed in this study (Supplementary Tables S2 and S4). Additionally, raw data processing, which includes the construction of a rating curve and calculations of vertical change, may introduce numerical calculation errors. The results show that the correlation coefficients of annual formula equations are consistently over 0.95. To further enhance the scientific validity of the processed data, a 95 % confidence interval was applied to the results, providing an additional layer of statistical reliability.

3. Results

3.1. Temporal trends and spatial dynamics of salt marshes and bare flats in JiuDuan Shoal (2002–2022)

Over the past two decades, the salt marshes within JiuDuan Shoal have exhibited a significant expansion, with an average increase of 3.66 km^2/yr. The total area of salt marshes grew from 35.9 km^2 in 2002 to 103.3 km^2 in 2022 (Fig. 3A). Notably, divergent trends were observed between the Upper Shoal and Middle-Lower Shoal salt marshes. The salt marshes in the Middle-Lower Shoal experienced an average expansion rate of 3.06 km^2/yr, while the Upper Shoal demonstrated a more modest seaward expansion rate of 0.38 km^2/yr (Fig. 3B). Consequently, the total salt marsh area increased by 191 % in the Upper Shoal and by 291 % in the Middle-Lower Shoal by 2022 compared to 2002, highlighting a more pronounced expansion in the Middle-Lower Shoal (Fig. 3A).

In addition, the salt marsh fringe, characterized by extensive intertidal bare flats exceeding 3 km, underwent two distinct phases of change from 2002 to 2022 (Fig. 3C). Between 2002 and 2014, the bare flats area remained relatively stable, averaging approximately 63.9 km2. However, from 2014 to 2022, a net reduction was observed, with an annual reduction rate of 2.16 km2, resulting in the bare flats area diminishing to 84 % of their 2014 extent (Fig. 3C). Furthermore, the average bare flat areas in the Upper Shoal and Middle-Lower Shoal were approximately 7.3 km2 and 54.6 km2, respectively, from 2002 to 2014. These areas experienced gradual decreases from 2014 to 2022 at annual rates of 0.52 km2 and 2.36 km2, respectively (Fig. 3C). These findings underscore significant ecological transformations in the JiuDuan Shoal, with implications for the region's biodiversity and habitat dynamics.

3.2. Expansion patterns of native and invasive salt marshes

The vegetation within the salt marshes of JiuDuan Shoal is primarily categorized into native species, including *Phragmites australis*, *Scirpus mariqueter*, and the invasive species *S. alterniflora*. In 2001, the Upper Shoal salt marshes were predominantly covered with native vegetation, while *S. alterniflora* was sparsely distributed in the center of the Middle-Lower Shoal (Fig. 4A). Subsequently, the native vegetation in the Upper Shoal exhibited radial expansion seaward, notably toward the northwest and southeast. *S. alterniflora* in the Middle-Lower Shoal expanded at a rate of 3.07 km^2/yr, increasingly encroaching on areas typically reserved for native vegetation growth over the past two decades. Although the native vegetation in the Middle-Lower Shoal continued to expand seaward, it did so at a slower rate than *S. alterniflora* (Fig. 4B–H). By 2014, *S. alterniflora* had almost completely overtaken the Middle-Lower Shoal salt marshes, with native vegetation confined to the central and tail areas of the shoal (Fig. 4F). By 2021, the distribution of *S. alterniflora* extended to the northern side of the Upper Shoal, with its area increasing from 2.96 km^2 in 2001 to 66.8 km^2 in 2021 (Fig. 4H and I). Additionally, from 2001 to 2021, the margins of *S. alterniflora*

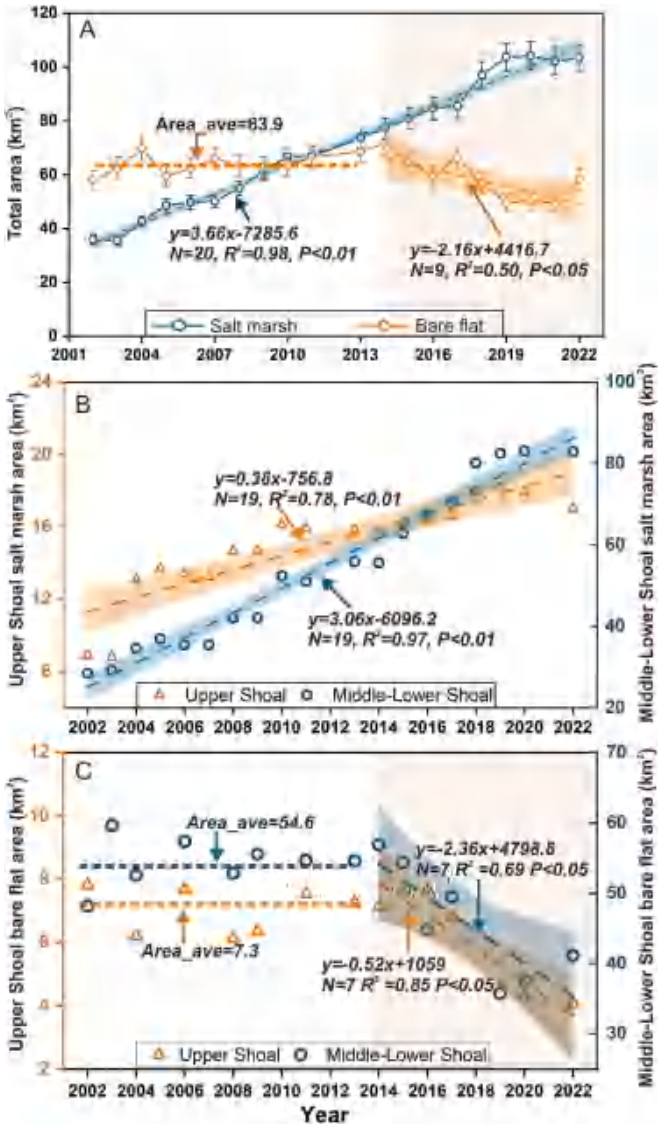

Fig. 3. Variations in the annual areas of salt marshes and bare flats at JiuDuan Shoal from 2002 to 2022. A. Total area of salt marshes and bare flats over the study period; B. Area of salt marsh in the Upper shoal and Middle-Lower Shoal; C. Area of bare flats in the Upper shoal and Middle-Lower Shoal.

extended seaward by over 7.11 km at the tail of the Middle-Lower Shoal, facilitating further expansion of the salt marshes.

3.3. Seaward expansion dynamics of salt marshes and bare flats

The salt marshes in JiuDuan Shoal exhibited seaward expansion in the last 20 years (Fig. 5A–D). In 2002–2022, the migration rates of salt marsh margins were 30.1 m/yr in the Upper Shoal, and 107.0 m/yr in the Middle-Lower Shoal, respectively (Fig. 6A and B). In the Upper Shoal, the salt marshes extended significantly to the northwest while experiencing retreat along the southern boundary. In contrast, the salt marshes in the Middle-Lower Shoal expanded in the northwesterly and southeasterly directions from 2002 to 2022. The remarkable expansion seaward occurred on the head of the Upper Shoal and the tail of the Middle-Lower Shoal, with an expansion rate of over 200 m/yr (Fig. 6A and B). Overall, the spatial dynamics of the salt marshes can be characterized by consistent seaward expansion, localized landward erosion, and substantial growth at both ends of the JiuDuan Shoal.

In addition, the bare flats exhibited a general trend of seaward migration, albeit at lower rates compared to the salt marshes (Fig. 5E–H). Specifically, the bare flats' margins migration rates in the Upper Shoal and Middle-Lower Shoal were 13.6 m/yr, and 64.5 m/yr, respectively between 2002 and 2022 (Fig. 6C and D). During this period, the bare flats in the Upper Shoal primarily expanded northwestward, with limited siltation in a southeast direction and erosion occurring on the southern side. Meanwhile, the bare flats in the Middle-Lower Shoal have continued to expand, notably at both the head and tail of the shoal, with migration rates averaging 55.6 m/yr at the head and 268.9 m/yr at the tail. These observations suggest a pattern of northern expansion coupled with southern erosion in the spatial dynamics of the bare flats. Moreover, the salt marshes and bare flats in JiuDuan Shoal have exhibited a general trend of northeasterly and southwesterly expansion, resulting in the narrowing of the tidal channel between the Upper Shoal and Middle-Lower Shoal (Fig. 5). Notably, the average width of this tidal channel decreased from 1.2 km in 2001 to 0.5 km in 2021.

3.4. Vertical accretion dynamics of salt marshes and bare flats

The salt marshes in JiuDuan Shoal exhibited significant deposition trends between 2002 and 2022 with a total accretion of over 2 m and an annual siltation rate of 0.15 m/yr (Fig. 7). Nevertheless, the vertical change in the bare flats and the siltation of the salt marshes were not synchronized. From 2002 to 2014, the elevation of bare flats increased by 0.2 m, with an annual accretion rate of 0. 01 m/yr. However, after 2014, the bare flats transitioned from s state of accretion to erosion, resulting in a cumulative elevation loss of 0.5 m from 2014 to 2022, which indicates a vertical erosion rate of 0.07 m/yr. Thus, the vertical change of the bare flats can be characterized by a "deposition–erosion" cycle (Fig. 7), despite the continued increase in the accretion rate of the salt marshes.

The generalized elevation variation results reflect the ongoing deposition of salt marshes alongside the transformation of bare flats from a state of deposition to one of erosion. These findings are consistent with previous studies (Xie et al., 2006; Gao et al., 2010; Cheng et al., 2020). For example, Xie et al. (2006) reported a sedimentation rate of 0.007 m/yr in the bare flat of JiuDuan Shoal based on short-column analyses. Similarly, Gao et al. (2010) observed an increase in the maximum elevation of JiuDuan Shoal from 0.3 m in 1958 to 4.9 m in 2005, corresponding to an annual deposition rate of 0.10 m/yr based on field observations. However, recent studies do not provide updated measurements of the deposition rate for the tidal flats in JiuDuan Shoal. This study addresses this gap by providing current sedimentation rate data for the region, contributing valuable insights to the understanding of coastal dynamics in this study area.

4. Discussion

4.1. The impact of fluvial sediment dynamics on salt marsh and bare flat development

Fluvial sediment plays a crucial role in the development of salt marshes in mega-estuaries worldwide (Dunn et al., 2019; Dai, 2021). A reduction in sediment supply is often associated with salt marsh erosion in the estuarine environment (Syvitski et al., 2005; Anthony et al., 2015). For instance, the fluvial suspended sediment discharge in Changjiang Estuary has decreased dramatically from 4×10^8 t to less than 1×10^8 t over the past 50 years (Fig. 8A). Notably, following the operation of the Three Gorges Dam in 2003, the annual suspended sediment discharge declined from 2.8×10^8 t in 2002 to 0.7×10^8 t in 2022, reflecting a reducing rate of 6.8×10^6 t/yr (Fig. 8A). Despite this substantial decline in sediment supply, the salt marshes at JiuDuan Shoal expanded between 2002 and 2022, while the bare flats initially experienced growth followed by a modest decrease. Importantly, there is no substantial correlation between fluvial suspended sediment discharge and the areas of salt marshes and bare flats (Fig. 8B). Nevertheless, linear relationships exist between cumulative sediment load and

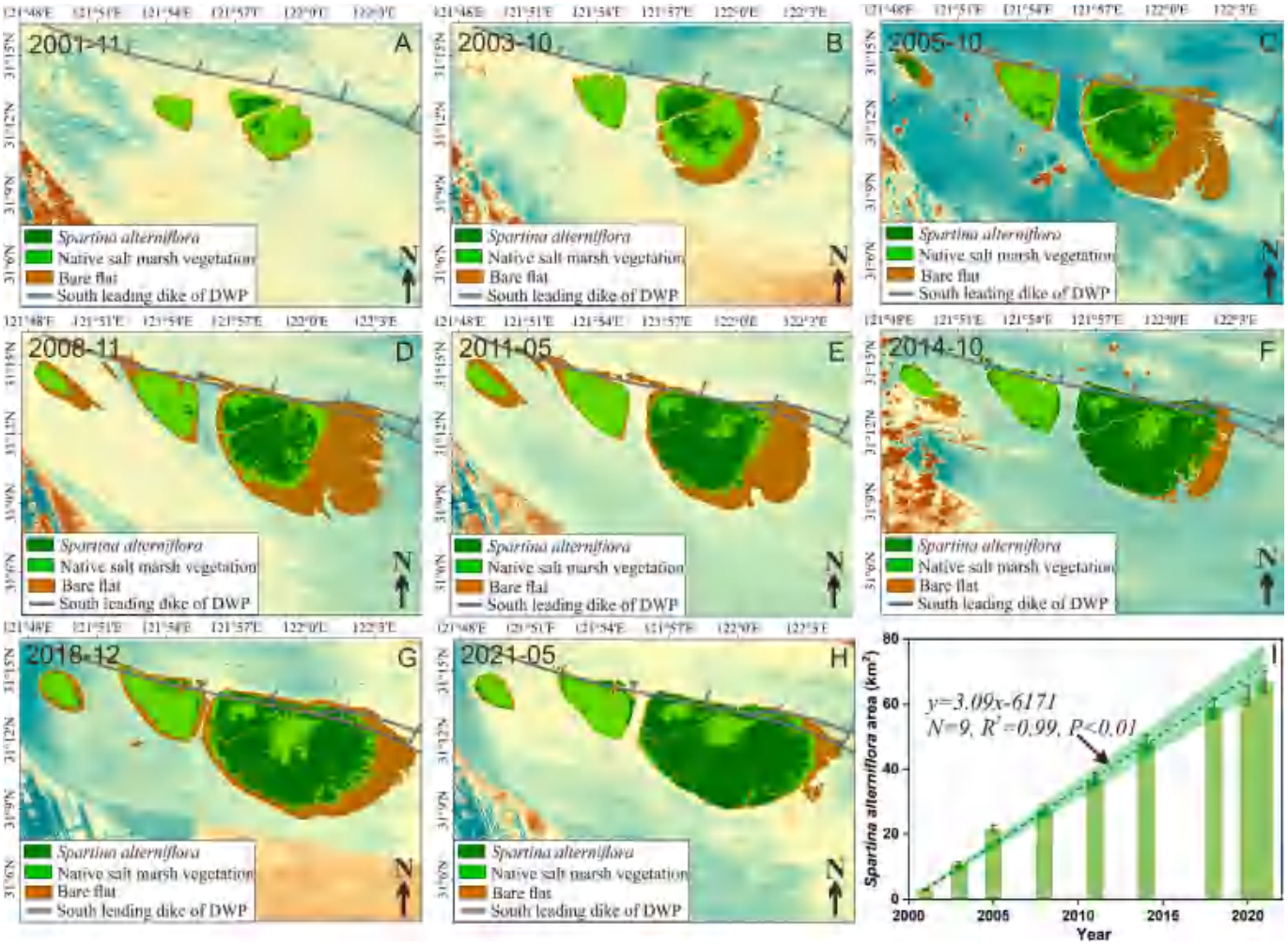

Fig. 4. Distribution variations of *Spartina alterniflora* at JiuDuan Shoal. A-H. Spatial distribution changes of *Spartina alterniflora* over time. I. Multi-year area changes of *Spartina alterniflora* within JiuDuan Shoal.

the areal extent of salt marshes and bare flats (Fig. 8C). This finding suggests that a decrease in fluvial sediment does not directly correlate with a proportional reduction in the area of salt marshes within JiuDuan Shoal from 2002 to 2022. However, fluvial sediment remains critical in sustaining salt marsh expansion over longer evolutionary timescales. The observed pattern of siltation followed by erosion in the bare flats may indicate a delayed response to the significant reduction in fluvial sediment supply. Additionally, morphodynamic processes operate over varying temporal scales (Zhou et al., 2017), which indicates the need for further investigation into the complex interactions between bare flat transformation and sediment supply reduction. Understanding these dynamics will enhance our knowledge of how anthropogenic influences, such as dam construction and sediment management practices, impact coastal ecosystems.

4.2. The role of suspended sediment supply in shaping salt marsh and bare flat resilience

An adequate sediment supply is critical for the siltation processes that underpin the development of salt marshes (Ladd et al., 2019). The JiuDuan Shoal, located between the South Passage and North Passage, is greatly influenced by the suspended sediment variations from these channels. Between 2002 and 2014, the suspended sediment concentration (SSC) in the South and North Passages fluctuated, averaging 1.24 kg/m^3 and 0.49 kg/m^3, respectively (Fig. 9). This occurred despite an obvious decline in suspended sediment discharge from upstream sources (Fig. 8). However, between 2014 and 2022, there was a marked decrease in the annual average SSC in both passages, dropping to 0.42 kg/m^3 in the South Passage and 0.29 kg/m^3 in the North Passage (Fig. 9). This decline coincided with a significant reduction in the bare flats of the JiuDuan Shoal, even as the expansion of salt marshes continued. Furthermore, a positive correlation between local SSC and the rate of change in the areas of both salt marshes and bare flats suggests the importance of local sediment dynamics in shaping their evolutionary trajectories. This observation aligns with findings from previous research (Li et al., 2016). The concurrent decrease in bare flats and the increase in salt marshes between 2014 and 2022 suggests that the reduction in SSC may have directly influenced the siltation processes affecting the bare flats. Conversely, salt marshes have demonstrated resilience by maintaining growth and effectively trapping sediment from adjacent waters, even under declining SSC conditions.

The dynamics of deposition and erosion in bare flats are closely linked to SSC, driven by flood-dominant current action. Previous works have also demonstrated that despite reductions in SSC, salt marshes can remain stable and even expand seaward (Leonardi et al., 2021; Zhang et al., 2021; Dai, 2021). This resilience is largely attributed to the capacity of salt marsh vegetation to reduce hydrodynamic energy and promote sediment deposition on adjacent tidal flats (Bouma et al. 2005). Consequently, under the current SSC conditions, the salt marshes at JiuDuan Shoal continue to expand seaward, while the bare flats are experiencing erosion.

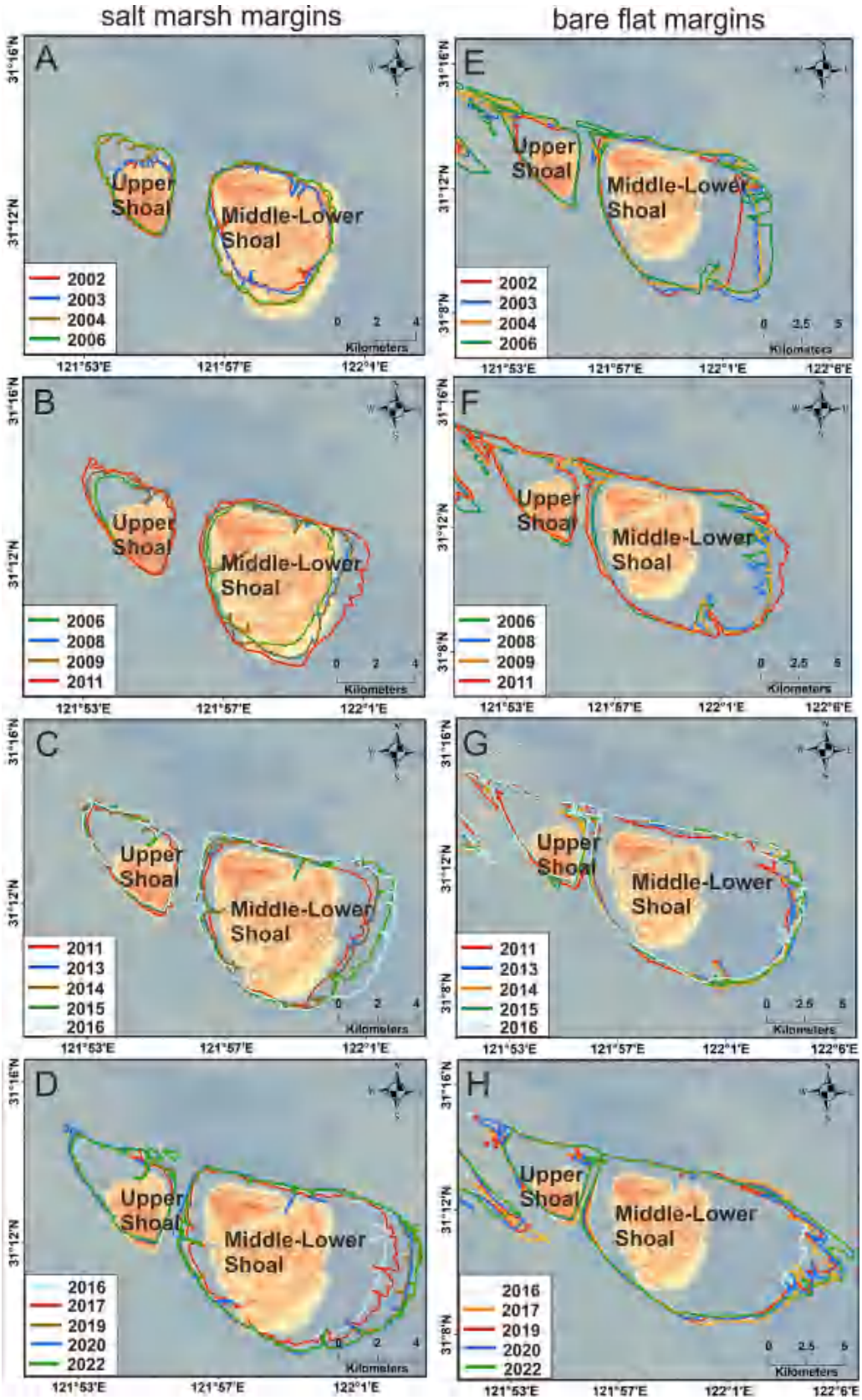

Fig. 5. Distribution of salt marsh and bare flat margins at JiuDuan Shoal from 2002 to 2022. A-D. Spatial distribution of salt marsh margins over the 20-year period. E-H. Spatial distribution of bare flat margins from 2002 to 2022.

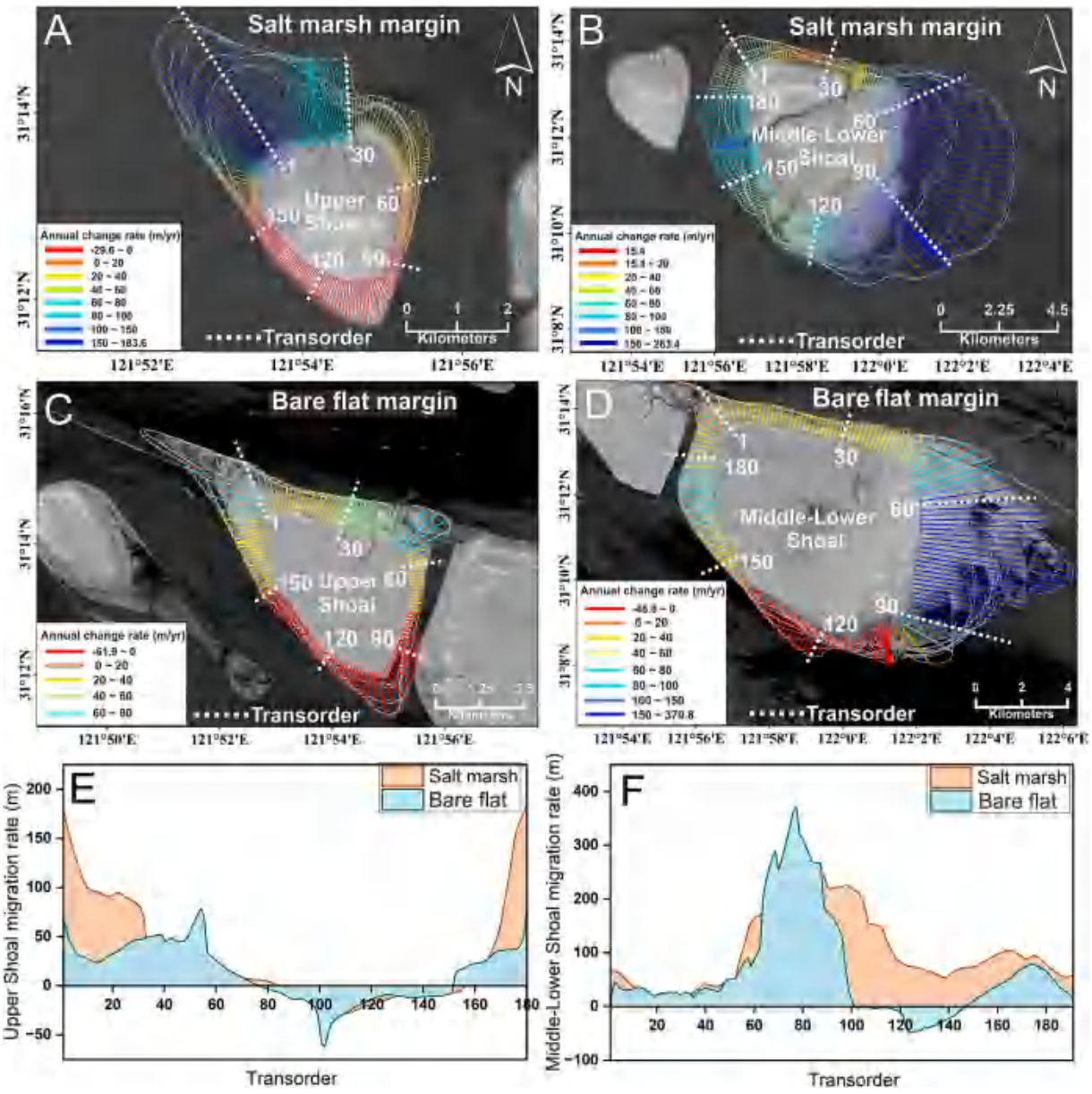

Fig. 6. Annual migration rates and spatial variations of salt marshes and bare flats at JiuDuan Shoal from 2002 to 2022. A-B. Spatial variations in the annual migration rates of salt marshes over the study period; C-D. Spatial variations in the annual migration rate of bare flats between 2002 and 2022; E-F. Statistic summary of migration rates for both salt marshes and bare flats.

4.3. Impacts of Deep Waterway Project on Hydrodynamics and coastal Ecosystem evolution

Between 2002 and 2022, significant infrastructural developments, namely the Deep Waterway Project (the Deep Waterway Project) and the Nanhui Shoal Reclamation Project, were implemented in the vicinity of JiuDuan Shoal, resulting in substantial alterations to the local hydrological environment and affecting the evolution of the shoal (Zhang et al., 2021). Specifically, the Deep Waterway Project has led to an upward trend in flow and sediment diversion ratios in the South Passage during both the flood and ebb tides from 2002 to 2011 (Fig. 10). This trend indicates an increase in the energy of the flow currents within the South Passage (Luo et al., 2023). Moreover, the Nanhui Shoal Reclamation Project has altered the orientation of the Nanhui shoreline from 144° prior to the project to 131° afterward, resulting in a northward deviation of the flow currents in the South Passage (Supplementary Fig. S6). The intensified northward flood tidal current has resulted in increased scouring along the southern edge of the JiuDuan Shoal. This is evidenced by the significant reduction in the distance between the −2 m and −5 m bathymetric contours at the southern end of the shoal, which decreased from approximately 4.9 km to 0.15 km, underscoring the impact of the enhanced flood tidal current from the South Passage (Fig. 1C).

Furthermore, since 2011, the Deep Waterway Project has resulted in more concentrated flow paths in the North Passage (Supplementary Fig. S7). The predominant tidal current directions have been confined to the main channel of the North Passage, thereby reducing lateral scouring along the JiuDuan Shoal. On the northern side of the shoal, the south training jetty acts as a protective barrier against strong hydrodynamic forces, thereby promoting sediment deposition in this area. This altered hydrodynamic environment has facilitated the expansion of salt marshes and supported the northwestward expansion of JiuDuan Shoal. These findings highlight the complex interplay between human interventions and natural sediment dynamics, emphasizing the need for ongoing

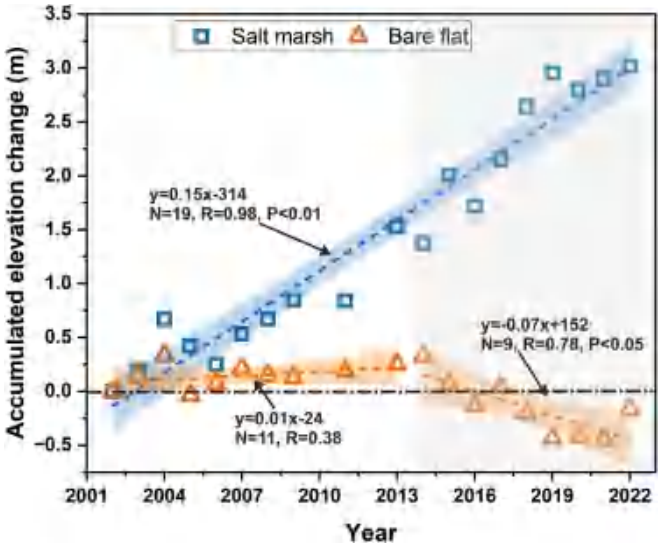

Fig. 7. Changes in Accumulated Elevation of Salt Marshes and Bare Flats at JiuDuan Shoal from 2002 to 2022.

monitoring and adaptive management strategies to ensure the sustainability of these critical coastal ecosystems.

4.4. Resilience of salt marshes and erosion risks in the Context of relative sea level rise

Salt marshes are at risk of erosional extinction when their vertical siltation rates fail to keep pace with regional relative sea level rise (Crosby et al., 2016). Over the past two decades, the annual average deposition rate within the JiuDuan Shoal salt marshes has reached an impressive 150 mm/yr. Conversely, the accretion rate of the bare flats has undergone a significant shift, declining from a positive rate of +10 mm/yr to a negative rate of −70 mm/yr. Previous studies, such as that by Wang et al. (2012), indicated that the average subsidence rate in the Changjiang Estuary is approximately 1.5 mm/yr. The average tidal level in Zhongjun has increased at the rate of 7.2 mm/yr (Fig. 11). Consequently, the relative sea level rise rate around JiuDuan Shoal is estimated to be about 8.7 mm/yr. Given the current sediment conditions, the siltation rates of the JiuDuan Shoal salt marshes significantly exceed the relative sea level rise.

Nevertheless, the bare flats at JiuDuan Shoal are currently experiencing erosion. Therefore, steep horizontal gradients in sediment trapping efficiency promote cliff formation at marsh edges (Fagherazzi et al., 2013). Progressive cliff elevation exacerbates salt marsh system instability by amplifying lateral erosion (Zhao et al., 2017). Concurrently, sea-level rise intensifies wave energy, increasing salt marsh erosion

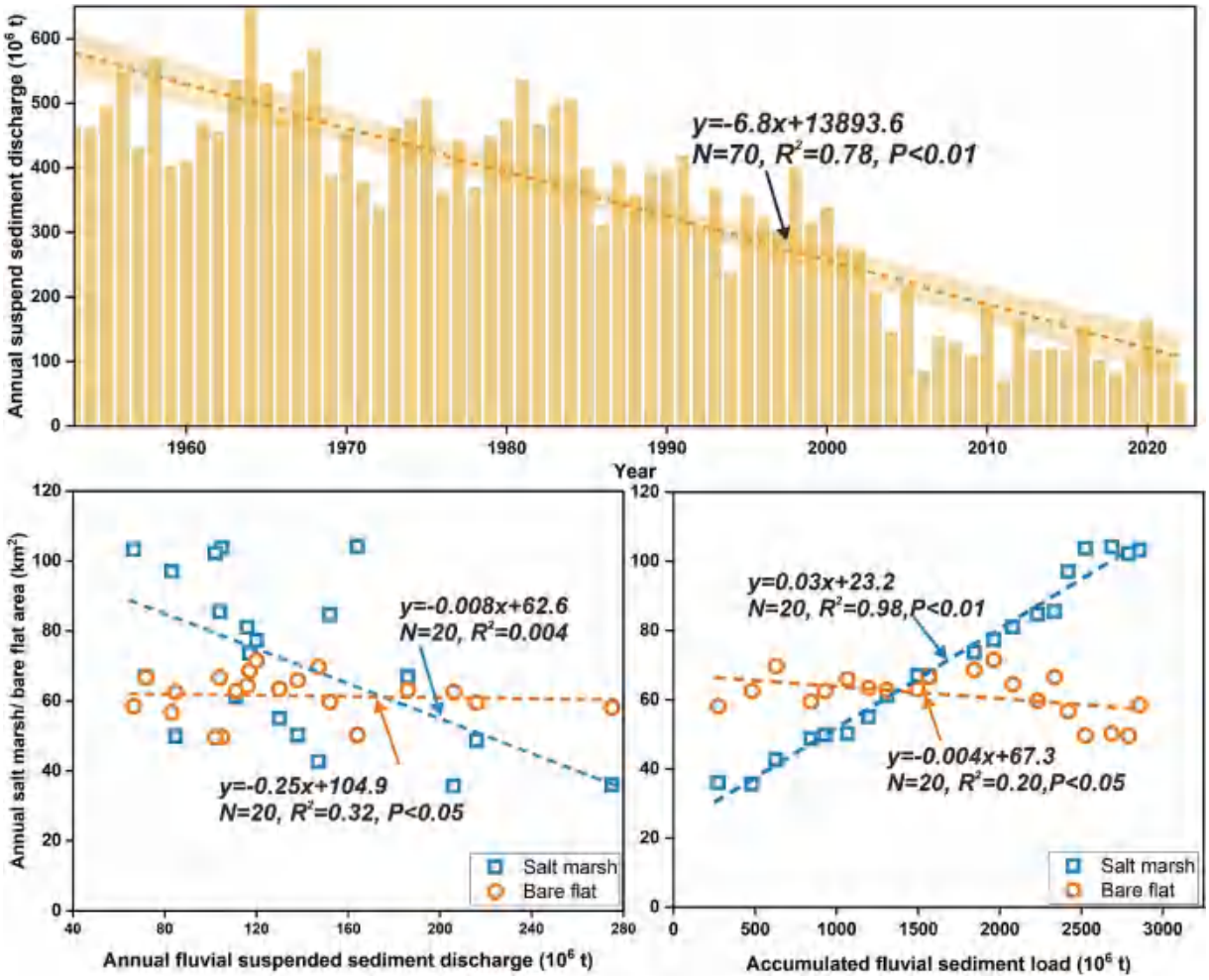

Fig. 8. Analysis of Fluvial Suspended Sediment Discharge and Its Impact on Coastal Landforms from 1950 to 2022. A. Annual fluvial suspended sediment discharge recorded from 1950 to 2022; B. Relationship between the annual areas of salt marshes and bare flats area and the corresponding fluvial suspended sediment discharge; C. Relationship between the annual areas of salt marshes and bare flats area and the accumulated fluvial suspended load.

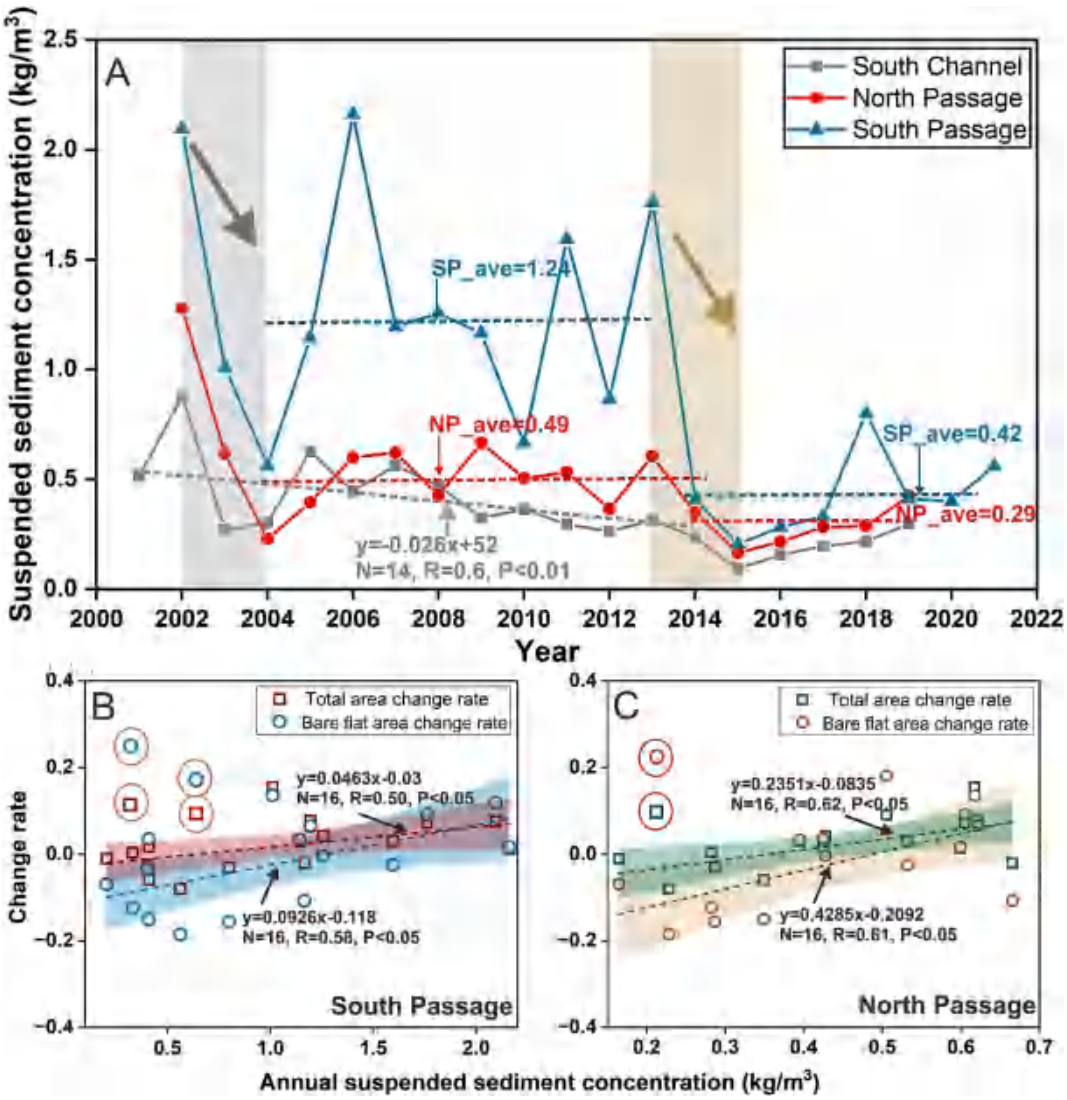

Fig. 9. Suspended Sediment Concentration and Its Relationship with Coastal Landform Changes from 2001 to 2021. A. Annual suspended sediment concentration in the South Channel, South Passage, and North Passage between 2001 and 2021; B. Relationship between the annual change rate of salt marshes/bare flats area and suspended sediment concentration in the South Passage; C. Relationship between the annual change rate of salt marshes/bare flats area and suspended sediment concentration in the North Passage.

susceptibility and compounding long-term degradation risks (Wang et al., 2024).

These findings highlight the necessity for continuous monitoring and management of suspended sediment dynamics in coastal ecosystems to ensure the sustainability of salt marshes and mitigate the impacts of sea level rise. Understanding the interplay between suspended sediment supply, accretion rates, and sea level dynamics is crucial for developing effective conservation strategies for vulnerable coastal habitats.

4.5. Temporal Morphodynamical patterns and ecological changes in JiuDuan Shoal

The dynamics of JiuDuan Shoal between 2002 and 2022 could be delineated into two distinct stages. In 2002, the original areas of salt marshes and bare flats within JiuDuan Shoal were recorded at 35.9 km^2 and 58.1 km2, respectively (Fig. 12A). The first stage, from 2002 to 2014, was characterized predominantly by deposition. During this period, the area of salt marshes in the JiuDuan Shoal experienced a continual increase at a rate of 3.66 km^2/yr, with an annual siltation rate reaching 0.15 m/yr (Fig. 12B). The area of bare flats in this shoal remained relatively stable, with a slight deposition rate of 0.01 m/yr. Moreover, significant horizontal expansion of JiuDuan Shoal occurred, from 2002 to 2014, marked by erosion along the southern edge and deposition on the northern side. The head of the Upper Shoal and the tail of the Middle-Lower Shoal emerged as primary sedimentation centers, marked by the consistent seaward extensions of these regions (Fig. 12B).

In the second stage, from 2014 to 2022, the salt marshes of JiuDuan Shoal continued to expand and experience vertical siltation while the bare flats transformed from slight deposition to erosion. The annual decrease in the area of the JiuDuan Shoal bare flats reached 2.2 km^2/yr, with a vertical erosion rate of 0.07 m/yr. During this period, the head of the Upper Shoal displayed landward retreat, while the salt marshes expanded northward (Fig. 12C). Conversely, the bare flats in the Middle-Lower Shoal contracted on the southern side while extending into the northwest and southeast regions (Fig. 12C). Additionally, the width of the tidal channel between the Upper Shoal and Middle-Lower Shoal narrowed significantly, from 1.2 km in 2001 to 0.5 km in 2021.

The invasion of *S. alterniflora* has notably altered the distribution of salt marsh communities. Initially, in 2002, *S. alterniflora* was sparsely distributed in the Middle-Lower Shoal (Fig. 12). However, it proliferated rapidly, eventually dominating most areas of the Middle-Lower Shoal, while native salt marsh vegetation became increasingly confined to the

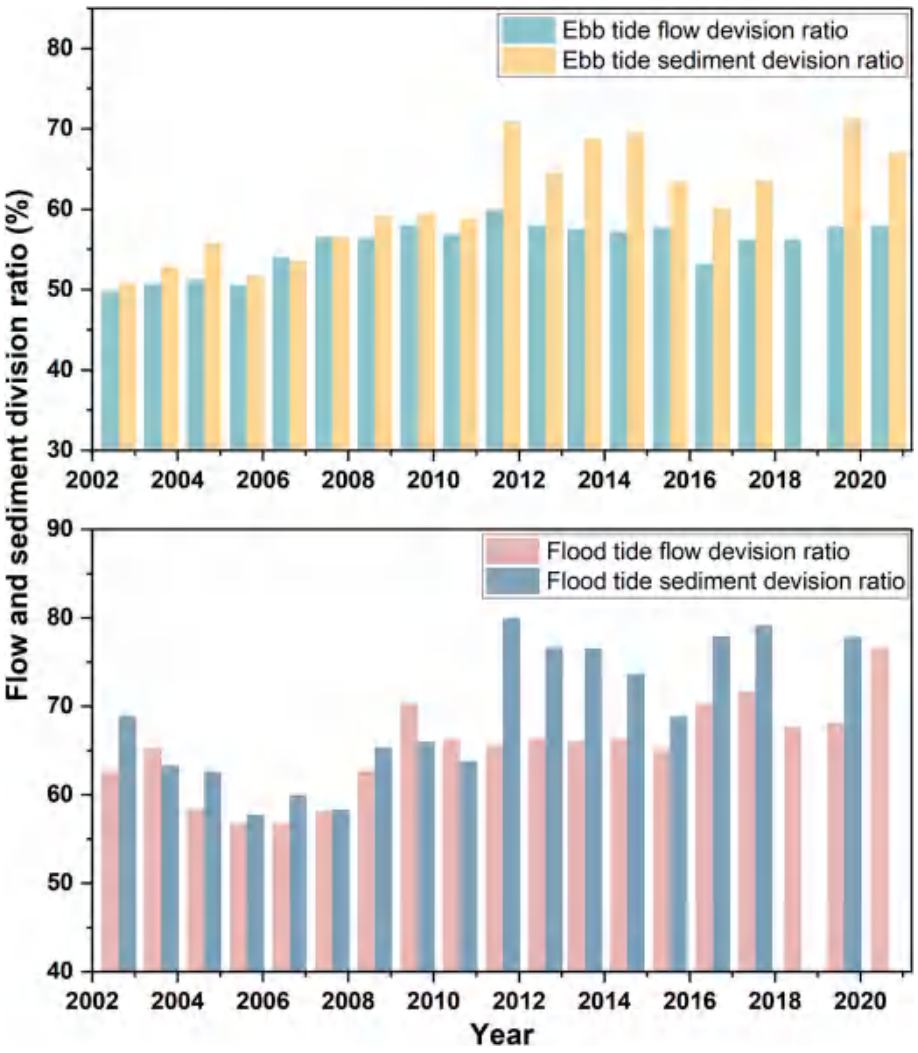

Fig. 10. Flow Dynamics and Sediment Diversion Ratios in the South Passage. A. Ebb tidal flow and sediment diversion ratio in the South Passage; B. Flood tidal flow and sediment diversion ratio in the South Passage.

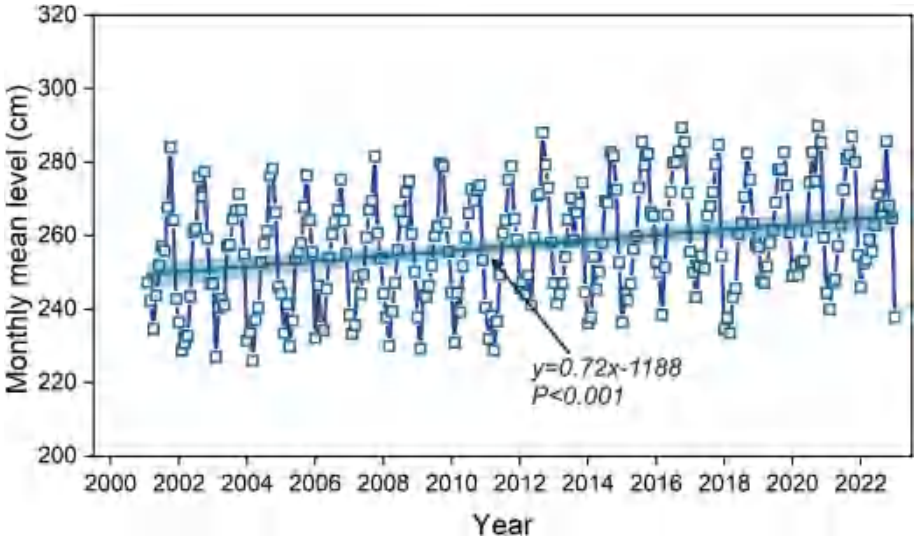

Fig. 11. Monthly average sea levels at Zhongjun tidal stations between 2001 and 2022.

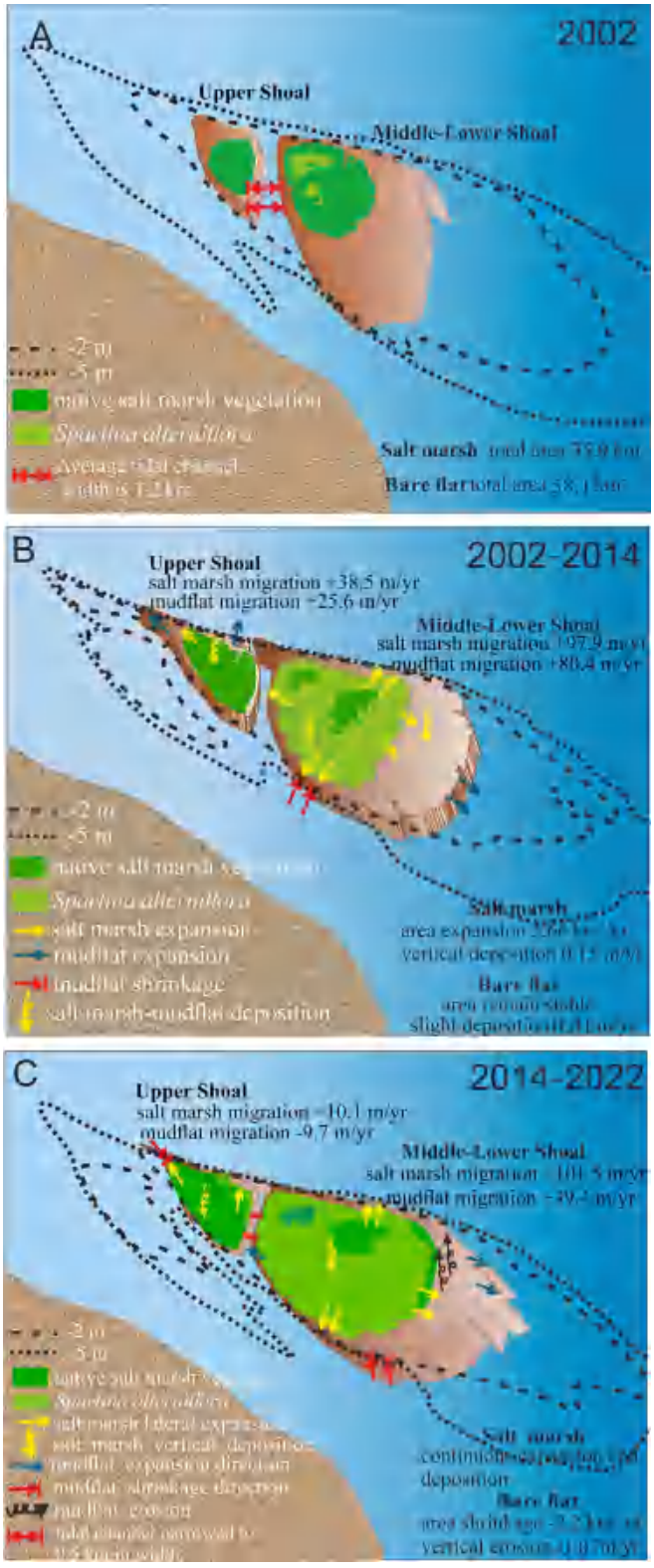

Fig. 12. Morphological changes of the Jiuduan Shoal between 2002 and 2022.

Upper Shoal and central regions of the Middle-Lower Shoal. More recently, *S. alterniflora* has begun to encroach upon the Upper Shoal, with remnants of native salt marsh vegetation persisting at the extremity of the Middle-Lower Shoal.

5. Conclusion

Salt marshes, as valuable natural habitats, are significantly influenced by both natural processes and anthropogenic activities. This study employed machine learning techniques to analyze the dynamics of JiuDuan Shoal, the largest uninhabited island in the Changjiang Estuary, over a two-decade period from 2002 to 2022. The key findings are summarized as follows:

The salt marshes of JiuDuan Shoal expanded at an average rate of 3.66 km^2/yr, accompanied by an annual vertical deposition rate of 0.15 m/yr. In contrast, the area of bare flats maintained approximately 63.9 km^2 from 2002 to 2014, but experienced net erosion at a rate of 2.16 km^2/yr between 2014 and 2022. Vertical changes in the bare flats shifted from a slight deposition rate of 0.01 m/yr during the first period (2002–2014) to erosion at −0.07 m/yr in the latter period (2014–2022).

The vegetation composition within the salt marshes underwent a significant alteration from 2002 to 2022. Initially, in 2001, native species dominated the Upper Shoal, while *S. alterniflora* was limited to the center area of the Middle-Lower Shoal. However, the invasive species *S. alterniflora* expanded dramatically at a rate of 3.07 km^2/yr, progressively displacing native vegetation. By 2021, *S. alterniflora* had largely taken over the Middle-Lower Shoal and extended into the tail of the Upper Shoal, with its coverage increasing from 2.96 km^2 to 66.8 km^2, thereby substantially contributing to overall salt marsh expansion.

The salt marshes in JiuDuan Shoal exhibited a significant seaward migration from 2002 to 2022, with migration rates of 30.1 m/yr in the Upper Shoal and 107.0 m/yr in the Middle-Lower Shoal, respectively. This expansion was primarily observed at the head of the Upper Shoal and the tail of the Middle-Lower Shoal. The bare flats showed deposition in the northern region and erosion in the southern region, with average migration rates of 13.6 m/yr in the Upper Shoal and 64.5 m/yr in the Middle-Lower Shoal between 2002 and 2022.

Despite a reduction in fluvial sediment supply, the relatively stable estuarine SSC has facilitated the continued seaward expansion of salt marshes in JiuDuan Shoal. The implementation of the Deep Waterway Project has increased tidal current energy in the South Passage and altered the tidal flow and direction in both the South and North Passages. These changes have shaped the spatial pattern of deposition and erosion within JiuDuan Shoal. Meanwhile, the increasing disparity in vertical siltation rates between salt marshes and their adjacent bare flats is promoting the development of cliffs along marsh edges. Projected sea-level rise is expected to exacerbate these dynamics, increasing the risk of lateral erosion and structural collapse in the salt marshes.

These findings underscore the dynamic nature of salt marsh ecosystems and the complex interplay of environmental factors driving their evolution. Sustained monitoring and adaptive management strategies are crucial to preserving these vital habitats in the face of ongoing environmental change.

CRediT authorship contribution statement

Yaying Lou: Writing – original draft, Methodology, Data curation. **Zhijun Dai:** Writing – review & editing, Validation, Supervision, Methodology. **Xuefei Mei:** Writing – review & editing, Resources, Methodology. **Huabing Shi:** Writing – review & editing, Validation, Supervision. **Hui Dong:** Resources, Methodology, Data curation. **Jinping Cheng:** Writing – review & editing, Validation, Supervision.

Declaration of competing interest

The authors declare that they have no known competing financial interests or personal relationships that could have appeared to influence the work reported in this paper.

Acknowledgments

This study was supported by the National Natural Science Key Foundation of China (42430406), National Natural Science Foundation of China (42306191), and the International Science and Technology Cooperation Fund Project of Shanghai, China (23230713800) Cooperation Fund Project (23230713800).

Appendix A. Supplementary data

Supplementary data to this article can be found online at https://doi.org/10.1016/j.ecolind.2025.114052.

Data availability

Data will be made available on request.

References

Anthony, E.J., Brunier, G., Besset, M., Goichot, M., Dussouillez, P., Nguyen, V.L., 2015. Linking rapid erosion of the Mekong River delta to human activities. Sci. Rep. 5, 14745.

Bouma, T.J., De Vries, M.B.D., Low, E., Peralta, G., Tanczos, I.C., van de Koppel, J., Herman, P.M.J., 2005. Trade-offs related to ecosystem engineering: a case study on stiffness of emerging macrophytes. Ecology 86, 2187–2199.

Campbell, A.D., Fatoyinbo, L., Goldberg, L., Lagomasino, D., 2022. Global hotspots of salt marsh change and carbon emissions. Nature 612, 701–706.

Chapman, V.J., 1960. Salt Marshes and Salt Deserts of the World. Interscience publishers, New York.

Chen, J.Y., 1988. Report on the Comprehensive Survey of Shanghai's Coastal Zone and Sea Paint Resources. Shanghai, Shanghai Science & Technology Press. pp. 4–7. (In Chinese).

Chen, G., Jin, R., Ye, Z., Li, Q., Gu, J., Luo, M., Wu, J., 2022. Spatiotemporal mapping of salt marshes in the intertidal zone of China during 1985–2019. J. Remote Sens. https://doi.org/10.34133/2022/9793626.

Cheng, H.F., Xin, P., Liu, J., Gu, F.F., Wang, W., Han, L., 2020. Morphological evolution and dynamic mechanics of the Jiuduansha Shoal (China) during 1959—2018. Adv. Water Sci. 30 (4), 492–501. In Chinese with English abstract.

Chen, J.Y., Li, D.J., Jin, W.H., 2001. Eco-engineering of Jiuduansha Island Caused by Pudong International Airport Construction. Eng. Sci. 3 (4), 3–8. In Chinese with English abstract.

Crosby, S.C., Sax, D.F., Palmer, M.E., Booth, H.S., Deegan, L.A., Bertness, M.D., Leslie, H. M., 2016. Salt marsh persistence is threatened by predicted sea-level rise. Estuar. Coast. Shelf. s. 181, 93–99.

Dai, Z.J., 2021. Changjiang riverine and estuarine hydro-morphodynamic processes, In the Context of Anthropocene Era. Springer Press.

Dunn, F.E., Darby, S.E., Nicholls, R.J., Cohen, S., Fekete, B.M., 2019. Projections of declining fluvial sediment delivery to major deltas worldwide in response to climate change and anthropogenic stress. Environ. Res. Lett. 14 (8), 084034.

Fagherazzi, S., Mariotti, G., Wiberg, P., McGlathery, K., 2013. Marsh collapse does notrequire Sea Level rise. Oceanogr 26 (3), 70–77.

Fagherazzi, S., Mariotti, G., Leonardi, N., Canestrelli, A., Nardin, W., Kearney, W.S., 2020. Salt marsh dynamics in a period of accelerated sea level rise. J. Geophys. Res. Earth Surf. 125 (8), e2019JF005200.

Gao, A., Yamg, S.L., Li, G., Li, P., Chen, S.L., 2010. Long-term morphological evolution of a tidal island as affected by natural factors and human activities, the Yangtze estuary. J. Coast. Res. 26 (1), 123–131. In Chinese with English abstract.

Gedan, K.B., Silliman, B.R., Bertness, M.D., 2009. Centuries of human-driven change in salt marsh ecosystems. Annu. Rev Mar. Sci. 1, 117–141.

Ge, Z.M., Zhang, L.Q., Yuan, L., 2015. Spatiotemporal dynamics of salt marsh vegetation regulated by plant invasion and abiotic processes in the Yangtze estuary: observations with a modeling approach. Estuar. Coast. 38 (1), 310–324.

Ge, Y., Pan, H., Zhang, J., Zhang, D., Wu, J., 2020. Exotic Spartina alterniflora invasion changes temporal dynamics and composition of spider community in a salt marsh of Yangtze Estuary, China. Estuar. Coast. Shelf. s. 239, 106755.

Granse, D., Suchrow, S., Jensen, K., 2021. Long-term invasion dynamics of Spartina increase vegetation diversity and geomorphological resistance of salt marshes against sea level rise. Biol. Invasions 23, 871–883.

Huang, H.M., Zhang, L.Q., 2007. A study of the population dynamics of Spartina alterniflora at Jiuduansha shoals, Shanghai, China. Ecol. Eng. 29 (2), 164–172.

Horton, B.P., Shennan, I., Bradley, S.L., Cahill, N., Kirwan, M., Kopp, R.E., Shaw, T.A., 2018. Predicting marsh vulnerability to sea-level rise using Holocene relative sea-level data. Nat. Commun. 9, 2687.

Jankowski, K.L., Törnqvist, T.E., Fernandes, A.M., 2017. Vulnerability of Louisiana's coastal wetlands to present-day rates of relative sea-level rise. Nat. Commun. 8 (1), 1–7.

Jia, K., Jiang, W., Li, J., Tang, Z., 2018. Spectral matching based on discrete particle swarm optimization: A new method for terrestrial water body extraction using multi-. temporal Landsat 8 images. Remote Sens. Environ. 209, 1–18.

Kirwan, M.L., Temmerman, S., Skeehan, E.E., Guntenspergen, G.R., Fagherazzi, S., 2016. Overestimation of marsh vulnerability to sea level rise. Nat. Clim. Chang. 6 (3), 253–260.

Ladd, C.J., Duggan-Edwards, M.F., Bouma, T.J., Pagès, J.F., Skov, M.W., 2019. Sediment supply explains long-term and large-scale patterns in salt marsh lateral expansion and erosion. Geophys. Res. Lett. 46 (20), 11178–11187.

Laengner, M.L., Siteur, K., van der Wal, D., 2019. Trends in the seaward extent of saltmarshes across Europe from long-term satellite data. Remote Sens. 11, 1653.

Leonardi, N., Mei, X.F., Carnacina, I., Dai, Z.J., 2021. Marine sediment sustains the accretion of a mixed fluvial-tidal delta. Mar. Geol. 438, 106520.

Li, X., Liu, J.P., Tian, B., 2016. Evolution of the Jiuduansha wetland and the impact of navigation works in the Yangtze Estuary, China. Geomorphology 253, 328–339.

Lin, S.W., Li, X.Z., Yang, B., Ma, Y., Jiang, C., Xue, L., Yan, Z., 2021. Systematic assessments of tidal wetlands loss and degradation in Shanghai, China: from the perspectives of area, composition and quality. Glob. Ecol. Conserv. 25, e01450.

Liu, J., Feng, Q., Gong, J., Zhou, J., Li, Y., 2016. Land-cover classification of the Yellow River Delta wetland based on multiple end-member spectral mixture analysis and a Random Forest classifier. Int. J. Remote Sens. 37 (8), 1845–1867.

Luo, J.J., Dai, Z.J., Wang, J., Lou, Y.Y., 2023. Effects of human-induced riverine sediment transfer on deposition-erosion in the South Passage of the Changjiang (Yangtze) delta. J. Hydrol. 622 (Part B), 129714.

Murray, N.J., Phinn, S.R., Clemens, R.S., Roelfsema, C.M., Fuller, R.A., 2012. Continental scale mapping of tidal flats across East Asia using the Landsat archive. Remote Sens. 4 (11), 3417–3426.

Murray, N.J., Phinn, S.R., DeWitt, M., Ferrari, R., Johnston, R., Lyons, M.B., Clinton, N., Thau, D., Fuller, R.A., 2019. The global distribution and trajectory of tidal flats. Nature 565 (7738), 222–225.

Ouyang, Z., Gao, Y., Xie, X., Guo, H., Zhang, T., Zhao, B., 2013. Spectral discrimination of the invasive plant Spartina alterniflora at multiple phenological stages in a saltmarsh wetland. PLoS One 8, e67315.

Tognin, D., D'Alpaos, A., Marani, M., Carniello, L., 2021. Marsh resilience to sea-level rise reduced by storm-surge barriers in the Venice Lagoon. Nat. Geosci. 14 (12), 906–911.

Reed, D.J., 1988. Sediment dynamics and deposition in a retreating coastal salt marsh. Estuar Coast Shelf S 26 (1), 67–79.

Schieder, N.W., Walters, D.C., Kirwan, M.L., 2018. Massive upland to wetland conversion compensated for historical marsh loss in Chesapeake Bay, USA. Estuar. Coast. 41 (4), 940–951.

Schuerch, M., Spencer, T., Temmerman, S., Kirwan, M.L., Wolff, C., Lincke, D., McOwen, C.J., Pickering, M.D., Reef, R., Vafeidis, A.T., Hinkel, J., Nicholls, R.J., Brown, S., 2018. Future response of global coastal wetlands to sea-level rise. Nature 561 (7722), 231–234.

Syvitski, J.P., Vörösmarty, C.J., Kettner, A.J., Green, P., 2005. Impact of humans on the flux of terrestrial sediment to the global coastal ocean. Science 308 (5720), 376–380.

Wang, J., Gao, W., Xu, S.Y., Yu, L.Z., 2012. Evaluation of the combined risk of sea level rise, land subsidence, and storm surges on the coastal areas of Shanghai, China. Clim. Change 115, 537–558.

Wang, K., Wu, G., Liang, B., Shi, B., Li, H., 2024. Linking marsh sustainability to event-based sedimentary processes: Impulsive river floods initiated lateral erosion of deltaic marshes. Coast. Eng. 190, 104515.

Wei, W., Dai, Z.J., Mei, X.F., Liu, J.P., Gao, S., Li, S.S., 2017. Shoal morphodynamics of the Changjiang (Yangtze) estuary: Influences from river damming, estuarine hydraulic engineering and reclamation projects. Mar. Geol. 386, 32–43.

Xie, X.P., Fu, B.H., Wang, Z.Y., Shen, H.T., 2006. Formation and Evolution of the Jiuduansha Shoal at the Changjiang Estuary based on the Digitized Sea Chart and Multi-temporal Satellite Images. Quat. Sci. 26 (3), 391–396. In Chinese with English abstract.

Yang, J.J., Dai, Z.J., Lou, Y.Y., Mei, X.F., Fagherazzi, S., 2023. Image-based machine learning for monitoring the dynamics of deltaic islands in the Atchafalaya River Delta complex between 1991 and 2019. J. Hydrol. 623, 129814.

Zhang, K.Y., Dong, X.Y., Liu, Z.G., Gao, W.X., Hu, Z.W., Wu, G.F., 2019. Mapping Tidal Flats with Landsat 8 Images and Google Earth Engine: a Case Study of the China's Eastern Coastal Zone circa 2015. Remote Sens. 11, 924.

Zhang, X.D., Xie, R., Fan, D.D., Yang, Z.S., Wang, H.M., Wu, C., Yao, Y.H., 2021. Sustained growth of the largest uninhabited alluvial island in the Changjiang Estuary under the drastic reduction of river-discharged sediment. Sci. China-Earth Sci. 64 (10), 1687–1697.

Zhao, Y., Yu, Q., Wang, D., Wang, Y.P., Wang, Y., Gao, S., 2017. Rapid formation of marsh-edge cliffs, Jiangsu coast, China. Mar. Geol. 385, 260–273.

Zhou, Z., Coco, G., Townend, I., Olabarrieta, M., Van Der Wegen, M., Gong, Z., D'Alpaos, A., Gao, S., Jaffe, B.E., Gelfenbaum, G., He, Q., Wang, Y.P., Lanzoni, S., Wang, Z.B., Winterwerp, H., Zhang, C.K., 2017. Is "morphodynamic equilibrium" an oxymoron? Earth Sci. Rev. 165, 257–267.